

Experimental study of mass transfer from the surface of a spherical water droplet assisted by spark discharge plasma channel

© I.A. Shorstkii

Kuban State Technological University, Krasnodar, Russia
e-mail: i-shorstky@mail.ru

Received March 6, 2023

Revised May 23, 2023

Accepted May 25, 2023

The results of an experimental study of the water (vapor) molecules transfer from the surface of a spherical droplet towards the anode when a spark discharge plasma channel flows at atmospheric pressure air are presented. Distilled water and sodium chloride aqueous solution were used in the experiments. Using a high-speed amplitude amplifier with a monitor output, the discharge current and voltage waveforms were obtained for four experiments: a spark discharge, a spark discharge with a drop of distilled water, a spark discharge with a drop of sodium chloride aqueous solution and a spark discharge with a multi-pointed anode structure and a drop of distilled water. Microstructural and energy dispersion analysis data were obtained to confirm the mechanism of substance transfer and the location of water molecules in the electric current closure zone of the spark discharge plasma channel on an aluminum substrate of a flat anode.

Keywords: spark discharge, plasma channel, mass transfer, water droplet, dissociation of molecules, ion channel, kangaroo effect.

DOI: 10.61011/TP.2023.08.57262.38-23

Introduction

The influence of an external electric field on the evaporation processes of water microdroplets attracts the attention of many researchers due to a wide range of practical applications in electrical micro- and nanoelectromechanical systems. The electric field has a significant effect in many cases, ranging from heat transfer during film boiling [1] to the manipulation of ultra-small droplets using the ionic wind of a corona discharge [2]. For example, the presence of electric field has a significant impact on local heat transfer processes due to the formation of air bubbles and evaporation during boiling [3]. It was established that the practical application of the electric field to water droplet is used in various fields, such as microelectronics, electrostatic painting, electrical spray, nanoimprinting and others [4–7]. In the direction of „green“ development of basic sectors of the food industry, the use of low-temperature plasma is being developed, in which the electric discharge interacts with food product, the main component of which is moisture [8,9]. For such technologies the processes of heat and moisture transfer under conditions of electrophysical effect are fundamental. Therefore, from both a scientific and a practical point of view it is necessary to clearly understand the effect of the electric discharge on the processes of substance transfer from the surface of water droplet.

Despite the large number of studies on the behavior of water droplet in the electric field, the mechanisms of matter transfer when water droplet is in the electric discharge were not fully studied [2.5–7]. The main difficulties that researchers face when performing this type of scientific studies:

a) high speed of the gas discharge propagation and small scale of the experiment, in which it is difficult to obtain realistic experimental data;

b) it is impossible to consider the same models at the macro-, micro- and nanoscale.

As a rule, in modern literature the molecular dynamics simulation tools are used to solve such problems. The papers of some authors has demonstrated the possibility of using the latter when considering the issues of sprays creation and evaporation [10]. However, the simulation was carried out without the electric field or electric discharge presence. A retrospective search shows that when setting the problem of the electric field effect on the water droplet, a system is considered in which the water droplet is located on a solid substrate acting as an electrode.

Thus, the authors noted the significant effect of the water contact angle, the size of the water droplet and the polarity of the applied electric field on the evaporation processes [11]. Another group of authors examined the behavior of an ion-containing water droplet in the electric field, in which processes of internal vortices occurred [12].

The purpose of this paper is to experimentally examine the features of the matter transfer from the surface of a water spherical droplet, when interacting with the oncoming flow of drifting and diffusing electrons emitted by a thermionic emission source, which are part of the plasma channel of a spark discharge. The author puts forward a hypothesis about the „kangaroo effect“ as the ability of filamentary plasma of spark discharge at one of the stages of its evolutionary development to transport the molecular ion of water H_2O^+ in close proximity from its lateral surface, along the vector of the external electric field to the substrate

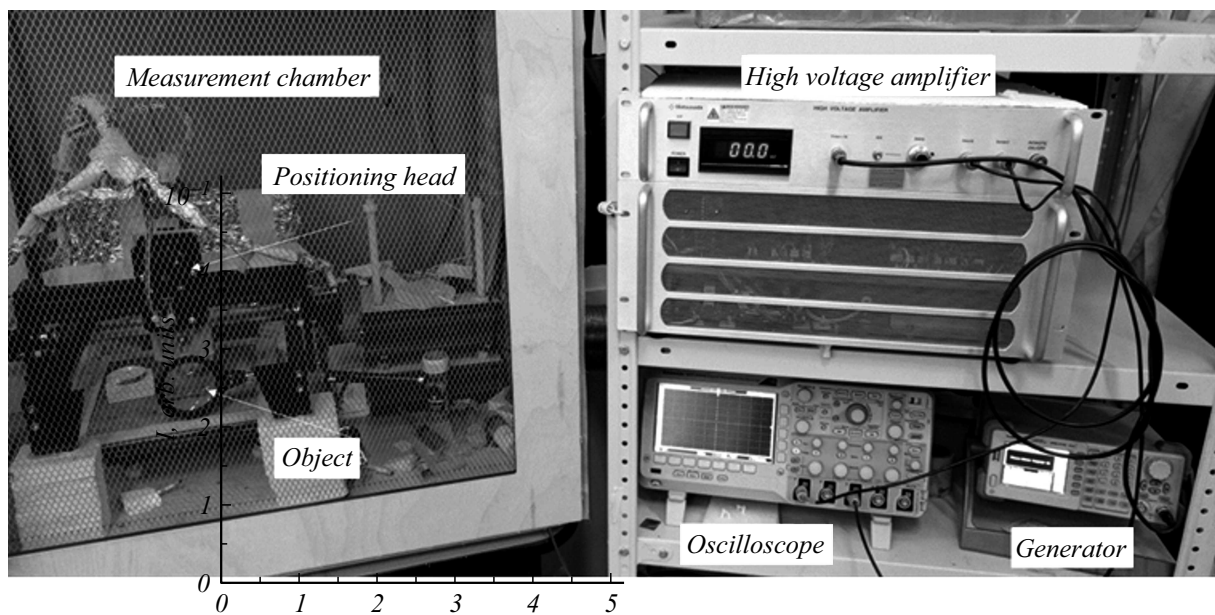


Figure 1. Laboratory set-up based on a Matsusada high-voltage amplifier.

of the anode plane, by analogy with the baby kangaroo transfer in the mother's pouch.

1. Measurement procedure and equipment

1.1. Electrode configuration and experimental set-up

To implement the experiment the laboratory set-up with an electrode system is used, see Fig. 1. A system consisting of function generator Agilent 33220A (Agilent Technologies, USA) and high-voltage amplifier Matsusada 20-B-20 (Matsusada Precision Inc, Japan) were used as a source of positive rectangular pulses. The maximum voltage at the amplifier output is 20 kV. The high-voltage amplifier is equipped with the ability to monitor current and voltage values at „monitor“ output. The characteristics of the shape, amplitude and duration of the pulse component of the discharge current and voltage were monitored using Tektronix TDS 220 digital oscilloscope.

Characteristics of the supplied pulse — rectangular positive pulse, duration 1 ms with repetition frequency 1 Hz. For all experiments the working gas — air at atmospheric pressure was used. All experiments were carried out in the presence of a thermoelectron emission source. The value of the active resistance of the filament (the source of thermoelectron emission) corresponded to $2\ \Omega$, and the value of the applied voltage was 1 V. The filament at one end is connected by an electrical circuit to ground potential and the cathode of the laboratory set-up. The anode is made of a cylindrical neodymium magnet and a conductive substrate made of an aluminum plate. According to the rule of behavior of charged particles, in the longitudinal

electric and magnetic fields of the laboratory set-up, when the poles of permanent magnets (electrodes) are oriented in the configuration S–N the charged particles move along a helical line.

To implement the task, 4 experiments were considered (Fig. 2):

— Experience A. A system of flat anode and flat cathode with thermoelectronic emission (TE) source in the form of a filament coil. The distance between TE source and the anode is 9.0 mm.

— Experience B. A system of flat anode, water droplet and flat cathode with TE source in the form of a filament coil. The distance between TE source and the anode is 9.0 mm. Center of water droplet is at distance of 4.5 mm from anode surface.

— Experience C. A system of flat anode, droplet of sodium chloride solution and flat cathode with TE source in the form of a filament coil. The distance between TE source and the anode is 9.0 mm. Center of water droplet is at distance of 4.5 mm from anode surface.

— Experience D. System of multi-point anode as per technology [13], water droplet and flat cathode with TE source in the form of filament coil. The feature of the formed multi-point surface is the presence of sharp ends formed by magnetically controlled Fe particles and the rotation of permanent magnet with residual magnetic induction 0.8 T using a motor (indicated as *M* in Fig. 2) and held by constant magnetic field of a dipole. The distance between TE source and the anode is 9.0 mm. Center of water droplet is at distance of 4.5 mm from anode surface.

In the proposed experiments the water droplet was placed using a dispenser into a round loop of polymer thread, where, under the effect of surface tension forces, it took a spherical shape. The internal diameter of the

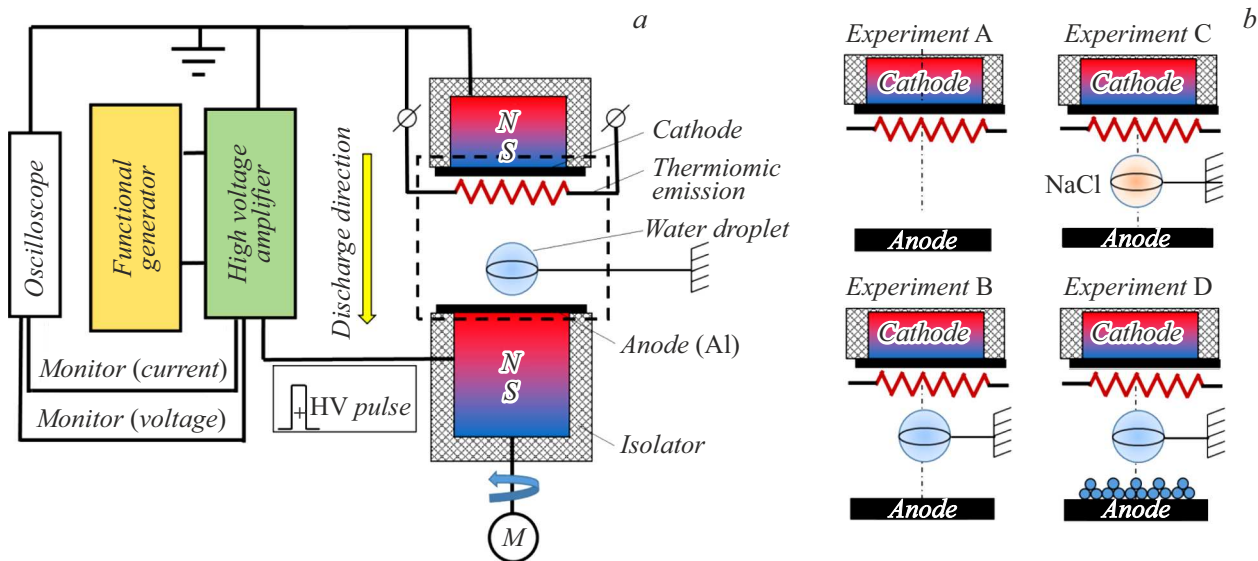


Figure 2. Scheme of the experimental set-up (not to scale) (a), and variation of experiments execution (b).

frame was 3 mm. Integral photographs of the discharge luminescence were obtained using a high-speed camera Nikon.

When the electric current of the plasma channel (total conduction and displacement current) is shorted to the aluminum substrate of the anode, Joule heat is released at the point of shortening. The result of Joule heat is the formation of a microcrater. After the water droplet was exposed to plasma channel of spark discharge in the zone of the anode plane, the microstructure of the surface of the aluminum anode substrate was studied to determine the geometric dimensions of the microcrater. Analysis of the chemical elements distribution at control points on an aluminum substrate was carried out using an EVO HD 15 scanning electron microscope (Zeiss, UK/Germany), equipped with an Aztec energy-dispersive microanalysis system. The study of the surface structures of the aluminum substrate was carried out at an accelerating voltage 10.0–30.0 kV.

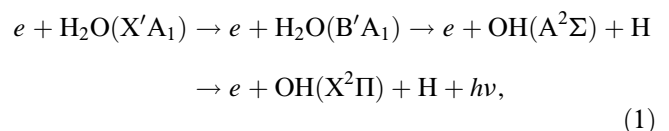
2. Process development scenarios

To describe the processes of water molecules transfer to the anode plane, a hypothesis is considered about the possibility of the molecular ion H_2O^- presence on the side surface of the plasma channel and the simultaneous movement of the latter to the anode along the external electric field vector (Fig. 3, stage 1). A situation similar to this was described during the drift of Al dust particle with an electron charge towards the anode in a previous work [14]. Thus, the process of water molecules transfer implies the presence of water molecules on the anode substrate in the microcrater radius zone.

To describe the processes of the spatial structure of the ion channel occurrence, two most likely scenarios are considered.

Scenario 1. Dissociative excitation of water molecules by thermalized electrons having a thermalization energy equal to the ionization energy of water molecule

Upon collision with thermalized electrons (Fig. 3, stage 2), which have thermalization energy equal to the ionization energy, the water molecule H_2O delivered to the anode disintegrates into a hydrogen atom H, which remains in the ground electronic state (unexcited) and the hydroxyl radical OH in the excited state ($\text{A}^2\Sigma$). This scenario is described by equation [15,16]:



where $\text{X}'\text{A}_1$ — normal state of a water molecule at room temperature, $\text{B}'\text{A}_1$ — linear state of water molecules, $\text{A}^2\Sigma$ — excited state of water molecule, $\text{X}^2\Pi$ — one of the intermediate states during the transition from the excited state $\text{A}^2\Sigma$.

Scenario 2. Ohmic heating of the anode in the zone of an erosion crater from the shorting of the electric current of the spark discharge plasma channel

This scenario considers the possibility of water molecules dissociation due to the amount of heat released as result of local melting of the anode metal in the erosion crater zone from the shorting of the electric current of the spark discharge plasma channel. To form microcrater on the surface of the anode substrate, it is necessary that electric current flow through the current-receiving section of the anode surface, which will do work aimed at local melting of the anode substrate metal (Fig. 3, stage 2). The corresponding energy balance for melting the anode metal per 1 microcrater under adiabatic conditions has the

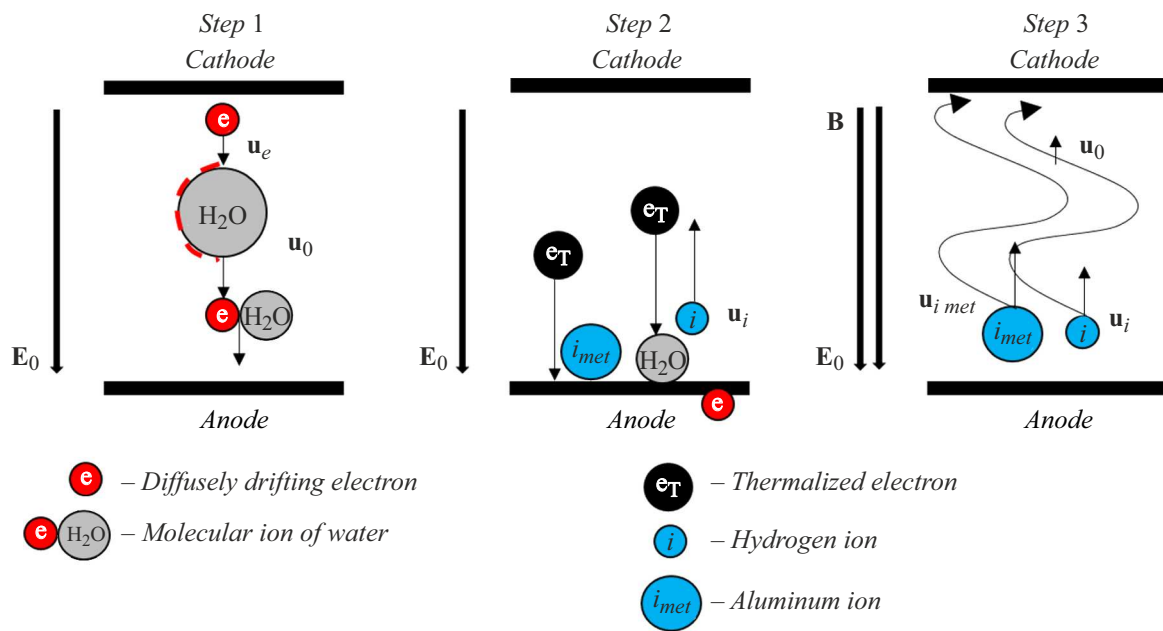


Figure 3. Schematic representation of the matter transfer from the surface of water spherical droplet when flowing around the spark discharge by plasma channel in longitudinal electric and magnetic fields: transfer of water molecular ion towards the anode by diffuse drifting electrons emitted by thermoelectric emission (stage 1), dissociation of water molecules from interaction with Joule heat released when the electric current of the plasma channel is shorted on the anode substrate (stage 2) and the drift of ions along a spiral trajectory in the longitudinal electric and magnetic fields towards the cathode, as a result of joint erosion of the metal of the anode substrate and dissociation of water molecules (stage 3).

following form [17,18]:

$$V_{mc}\rho Q_m = \left(\frac{I}{N}\right)^2 R\Delta t, \tag{2}$$

where $V_{mc} = \pi r 2l_{mc}$, r — microcrater radius, l_{mc} — its effective depth, ρ — density of the electrode material, Q_m — specific heat of fusion of the anode metal, I — current, N — number of microcraters, $R = \rho_e l_{mc} / \pi r^2$ — resistance of the volume element of the future microcrater, ρ_e — resistivity of the flat electrode material, Δt — time. The thermal conductivity of air is by more than two orders of magnitude less than the thermal conductivity of the anode material, and for the durations under consideration the heat transfer from the heated gas from the areas adjacent to the microcrater can be neglected [18]. Therefore, within the framework of the evaluations performed, only ohmic heating was taken into account as the main heating factor.

From expression (2) the microcrater radius can be determined [18]:

$$r = \sqrt[4]{\frac{\rho_e I^2 \Delta t}{\pi^2 \rho Q_m N^2}}. \tag{3}$$

The radius of the microcrater is a kind of target where molecular ions of water H_2O^+ are delivered, they drift in external electric field in the immediate vicinity of the plasma channel body. Thus, in the microcrater radius zone on the anode surface, the water molecule dissociation

is possible according to scenarios 1 and 2. Registration of the luminescence is assessed visually in the form of luminescence in the visible region of the spectrum according to expression (1).

During the experiment the resulting ion current is shorted on the current-collecting surface of the cathode plane. Thus, the thermoelement is a probe and is characterized by the surface area on which the ion current is shorted [15]. The appearance of the electric ion current in the interelectrode space leads to the formation of a volumetric spiral-shaped ion channel. The ion current concentration is characterized by the value at which the ion current saturation is observed and is determined by the formula [17]:

$$i_+ \approx 0.52 S e n_0 \sqrt{\frac{kT_e}{M_i}}, \tag{4}$$

where $e n_0$ — electron concentration on the current-collecting surface of the cathode, S — cathode probe area, T_e — electron temperature in energy units.

From expression (4) we can express the concentration of charges

$$n_0 \approx \frac{i_+}{0.52 S e v_+}, \tag{5}$$

where v_+ — the velocity of ions under the action of external electric field.

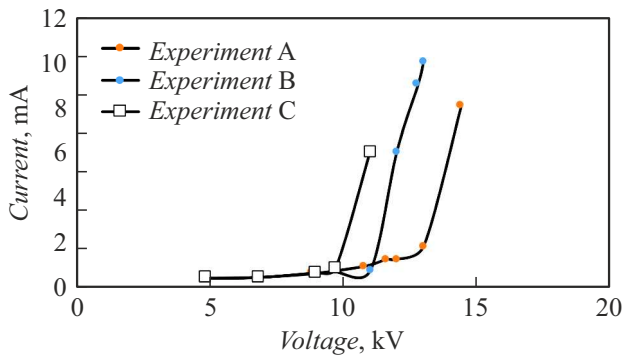


Figure 4. Current-voltage curve of the plasma channel of spark discharge in atmospheric air for experiments A–C.

3. Measurement results

3.1. Electrical characteristics of spark discharge plasma channel according to experiments A–C

On the current oscillograms for the experiments A–C, the delay in the increase in the electron current from the moment of voltage application is clearly noticeable at 600, 560 and 200 μs , respectively. One of the characteristic features of the plasma channel current is a long-term decrease in the current amplitude according to an exponential law. The beginning of the ion current increasing corresponds to the formation of a diffuse luminescence of spiral shape. A long-

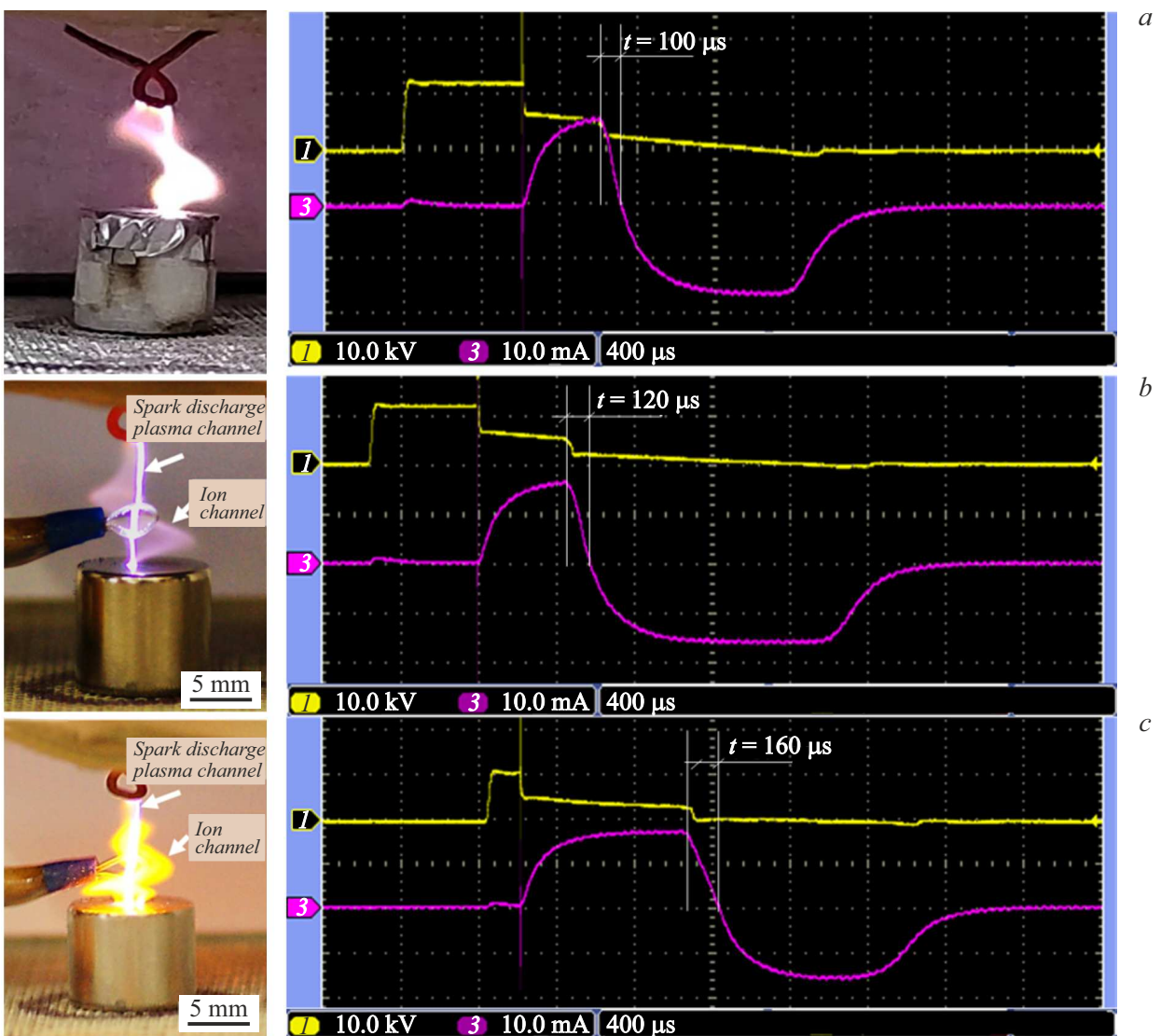


Figure 5. Visualization of voltage curve of the plasma channel for experiment A (a), B (b) and C (c). For experiments B and C, visualization is presented at the moment of the water spherical droplet flow around by the plasma channel of the spark discharge (a bright filament-shaped cord) and by ion channel (a spiral-shaped luminescence). Vertical scale: voltage — 10 kV/div (curve 1), current — 10 mA/div (curve 3); horizontal 400 μs /div.

term decrease in amplitude can be attributed to the result of the drift of the molecular ion ($H_2O, -e$) in the immediate vicinity of the of the spark discharge plasma channel in external electric field and the electric current shorting within the microcrater radius.

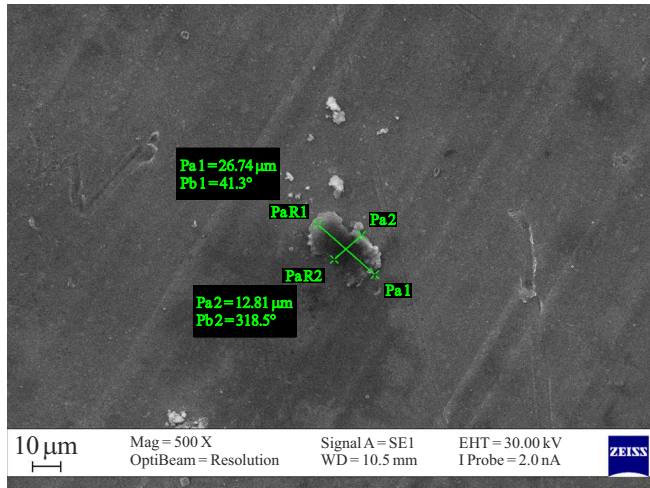


Figure 6. Visualization of microcrater on the surface of aluminum substrate as a result of the experiment carried out according to experiment B.

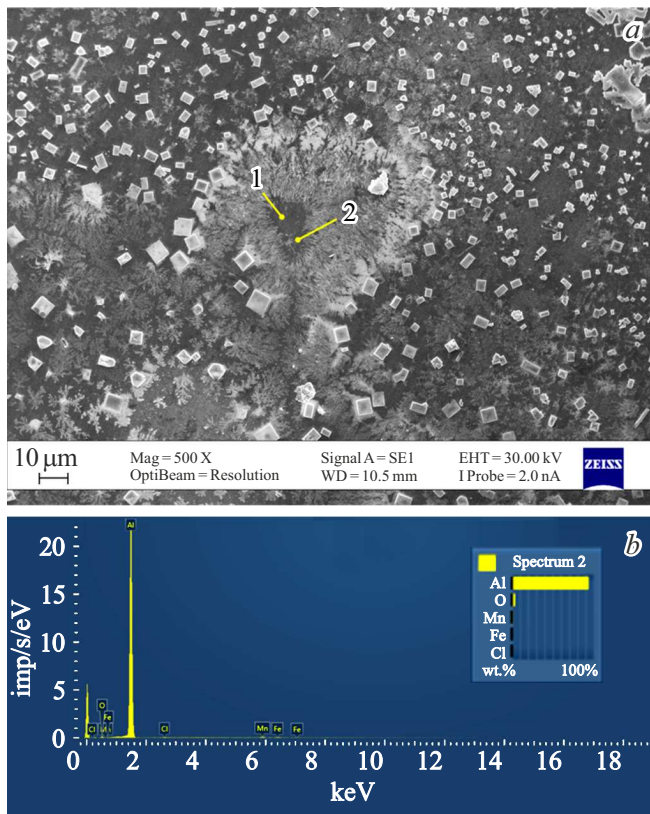


Figure 7. Microstructure of aluminum substrate according to the result of experiment B for water droplet with sodium chloride (a) and the spectrum of chemical elements distribution at point 2 (b).

Quantitative composition of chemical elements at control points in accordance with Fig. 7

Spectrum name	O	Al	Cl	Mn	Fe	Total
Spectrum of point 1		97.72		1.34	0.94	100
Spectrum of point 2	4.23	93.57	0.37	1.24	0.59	100

Fig. 4 shows the current-voltage curves (CVC) of the spark discharge plasma channel in the laboratory system under consideration. The obtained CVCs demonstrate a characteristic dependence for the spark discharge plasma channel at low current values. When comparing the CVCs for experiments A–C, a decrease in the breakdown voltage of the interelectrode space between the anode and cathode in the laboratory set-up is observed, from value of 14.2 kV for experiment A to value of 11.6 kV for experiment B, and 11.1 kV for experiment C. The decrease in the breakdown voltage is due to a change in the electrical conductivity of the interelectrode space as result of the presence of water droplet (experiment B) and sodium chloride solution (experiment C). For the experiments under consideration, Fig. 5 shows integral photographs of the discharge luminescence and the corresponding current and voltage oscillograms. In the integral photograph, two areas of luminescence are distinguished: electron current and diffuse luminescence of the spiral shape for all experiments performed. According to the law of motion of charged particles, in longitudinal electric and magnetic fields the trajectory of particle is a helical line. Note that the presence of sodium chloride solution in the interelectrode space caused a change in the color of the diffuse luminescence to a bright yellow color.

For a more detailed analysis of the hypothesis put forward about the presence of the „kangaroo effect“ the analysis of the aluminum substrate in the plasma channel shorting zone was carried out for the presence of microstructural changes. The surface of the aluminum substrate (anode) according to experiment B from scanning electron microscope is shown in Fig. 6. Assuming for aluminum $\rho = 2.7 \cdot 10^3 \text{ kg/m}^3$, $Q_m = 3.9 \cdot 10^5 \text{ J/kg}$, $\rho_e = 2.7 \cdot 10^{-8} \Omega \cdot \text{m}$, $I = 14 \text{ mA}$ for $\Delta t = 240 \text{ ms}$ (with processing time 100 s), in accordance with expression (3) we obtain $r = 4.3 \mu\text{m}$. In this case, the diameter of the microcrater as a result of metal melting in Fig. 5 is $12.8 \mu\text{m}$. Considering the fact that detecting the presence of hydroxyl OH^- in the substrate area is a complex technical task, the substrate was analyzed according to experience C. To confirm the „kangaroo effect,, on the transfer of water molecules (H_2O^- molecular ion) to the microcrater zone of the anode plane, experiment B was modified. To do this, sodium chloride was added to the initial droplet of distilled water in an amount corresponding to concentration of 10% (experiment C). Fig. 7 shows an image obtained using the scanning electron microscope and

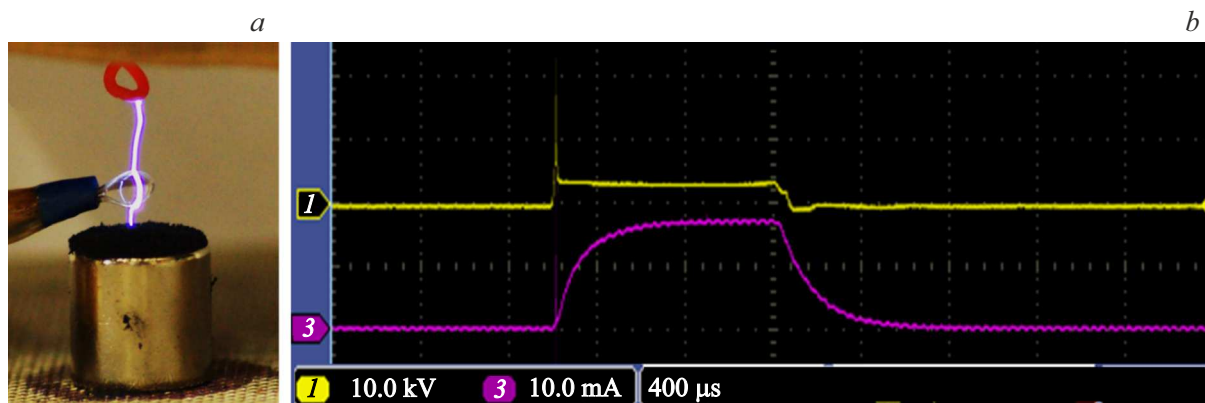


Figure 8. Integral photograph of spark discharge plasma channel using a multi-point anode structure (a) and an oscillogram of conduction current and voltage (b). Vertical scale: voltage — 10 kV/div (line 1), current — 10 mA/div (line 3); horizontally 400 μ s/div.

spectral analysis of the components distribution at selected control points on the anode substrate surface.

Energy-dispersive microanalysis shows the presence of chlorine in the microcrater zone (see Table) due to the implementation of the mechanism of matter transfer by the spark discharge plasma channel. Outside the microcrater zone there are pronounced NaCl salt crystals. To suppress the ion channel occurrence, it is possible to use multi-point anode surface in the form of magnetically controlled iron oxide particles Fe_3O_4 [19] (Fig. 8) based on experience D. This feature will create the opportunity to evaluate components transferred to the anode substrate without subsequent destruction by the resulting ion current (Fig. 8, b).

Conclusion

Visual observation of the electric current (total conduction current and displacement current) of the spark discharge plasma channel and the ion current of the ion channel when flowing around the water spherical droplet, according to the obtained oscillogram (Fig. 5), showed the absence of current break during the action time of 2.4 ms of the impulse applied from the high-voltage amplifier.

Outside the geometric boundaries of the water spherical droplet, the transfer of water (steam) molecules towards the anode is carried out by the „kangaroo effect“, when diffusing and drifting electrons transport water molecules (H_2O^-) along the external electric field vector towards the anode (Fig. 3, stage 1). The formation of a stable molecular ion is characterized by the effect of electron adhesion to the water molecule. Fluctuations associated with the growth of negative molecular ions lead to the formation of domains. The domain moves towards the anode at a speed that is less than the electron drift speed, which leads to an increase in the duration of the electric current curve (Fig. 5).

Upon reaching the anode surface, the electrons of the negative ion (H_2O^-) are shorted on the anode in the erosion crater zone, where the Joule heat released due to local melting of the metal from the action of spark

discharge allows dissociation of water molecules. The result is the formation of hydrogen molecule (H) and hydroxyl ion (OH^-) (Fig. 3, stage 2). Dissociation of water molecules is possible due to the thermal energy released as a result of the microcrater formation during melting of the anode substrate metal. The diameter of the crater on the surface of the anode substrate is a kind of target where water molecules (H_2O^-) are delivered, the molecules drift in an external electric field, being on the lateral boundary surface of the plasma channel body.

Based on the experimental data obtained, the rationale for the „kangaroo effect“, is determined by the presence of water molecules in the crater formation zone, as a result of the work of matter transfer near the side surface of the plasma channel. This fact is further confirmed by microstructural analysis and the spectrum of chemical components distribution (Fig. 3) at control points when using sodium chloride as part of the water droplet. The dissociation of water molecules with pronounced optical radiation indicates that the water molecule received a portion of thermal energy in the microcrater zone, where the luminescence of the excited hydroxyl ion OH^- is evaluated visually in the form of the luminescence lying in the visible region of the spectrum (stage 3, Fig. 3). The composition of the light quantum radiation also includes radiation quanta associated with the melting of the anode substrate metal.

It seems promising to suppress the occurrence of the ion channel through the use of multi-point anode surface in the form of magnetically controlled particles Fe_3O_4 . This feature will create the opportunity to evaluate components transferred to the anode substrate without subsequent destruction.

Funding

This study was supported financially by the Kuban Science Foundation, FSBEI of HE „KubSTU“ within the framework of the scientific project № MFI-P-20.1/40. The

studies were carried out using the equipment of the Center for Shared Use „Research Center for Food and Chemical Technologies“ of KubSTU (CKP_3111), the development of which is supported by the Ministry of Science and Higher Education of the Russian Federation (Agreement № 075-15-2021-679).

Conflict of interest

The author declares that he has no conflict of interest.

References

- [1] N. Sharma, G. Diaz, E. Leal-Quirós. *Intern. J. Thermal Sci.*, **68**, 119 (2013). DOI: 10.1016/j.ijthermalsci.2013.01.003
- [2] A. Hens, G. Biswas, S. De. *J. Chem. Phys.*, **143** (9), 094702 (2015). DOI: 10.1063/1.4929784
- [3] J. Kornev, N. Yavorovsky, S. Preis, M. Khaskelberg, U. Isaev, B.N. Chen. *Ozone: Sci. Engineer.*, **28** (4), 207 (2006). DOI: 10.1080/01919510600704957
- [4] M. Damak, K.K. Varanasi. *Sci. Adv.*, **4** (6), 5323 (2018). DOI: 10.1126/sciadv.aao5323
- [5] A.A. Fedorets, L.A. Dombrovsky, E. Bormashenko, M. Nosonovsky. *Intern. J. Heat Mass Transfer.*, **113**, 712 (2019). DOI: 10.1016/j.ijheatmasstransfer.2018.12.160
- [6] P.M. Ireland, C.A. Thomas, B.T. Lobel, G.B. Webber, S. Fujii, E.J. Wanless. *Frontiers Chem.*, **6**, 280 (2018). DOI: 10.3389/fchem.2018.00280
- [7] D.N. Gabyshev, A.A. Fedorets, O. Klemm. *Aerosol Sci. Technol.*, **54** (12), 1556 (2020). DOI: 10.1080/02786826.2020.1804522
- [8] I. Bashkir, T. Defraeye, T. Kudra, A. Martynenko. *Food Engineer. Rev.*, **12** (4), 473 (2020). DOI: 10.1007/s12393-020-09229-w
- [9] I. Shorstkii, E. Koshevoi. *Chem. Engineer.*, **3** (4), 91 (2019). DOI: 10.3390/chemengineering3040091
- [10] B.B. Wang, X.D. Wang, Y.Y. Duan, M. Chen. *Intern. J. Heat Mass Transfer.*, **73**, 553 (2014). DOI: 10.1016/j.ijheatmasstransfer.2014.02.034
- [11] V. Vancauwenberghe, P. Di Marco, D. Brutin. *Colloids Surfaces A: Physicochem. Engineer. Aspects.*, **432**, 50 (2013). DOI: 10.1016/j.colsurfa.2013.04.067
- [12] Q. Brosseau, P.M. Vlahovska. *Phys. Rev. Lett.*, **119** (3), 034501 (2017). DOI: 10.1103/PhysRevLett.119.034501
- [13] I.A. Shorstkii, N. Yakovlev. *Inorgan. Mater.: Appl. Research.*, **11** (5), 1236 (2020). DOI: 10.1134/S2075113320050317
- [14] I.A. Shorstkii. *Tech. Phys.*, **91** (8), 1 (2022). DOI: 10.21883/JTF.2021.08.51105.4-21
- [15] A.V. Bernackij, V.N. Ochkin, O.N. Afonin. *Fizika Plazmy*, **41** (9), 767, (2015). (in Russ.)
- [16] V.N. Ochkin. *Spectroscopy of Low Temperature Plasma* (WILEY-VCH, Weinheim, 2009)
- [17] Yu.P. Raizer. *Fizika gazovogo razryada* (Intellekt, M., 2009) (in Russian).
- [18] E.K. Baksht, O.M. Blinova, M.V. Erofeev, V.I. Karelin, V.S. Ripenko, V.F. Tarasenko, M.A. Shulepov, *Plasma Physics Reports*, **42** (9), 876 (2016).
- [19] I.A. Shorstky, M.D. Sosnin. Patent RF № 2789539. (in Russian)

Translated by I.Mazurov